Spectrochimica Acta Part A 83 (2011) 200–206

Contents lists available at ScienceDirect

Spectrochimica Acta Part A: Molecular and Biomolecular Spectroscopy

journal homepage: www.elsevier.com/locate/saa

A physiochemical study of azo dyes: DFT based ESIPT process

Jayaraman Jayabharathi *, Venugopal Thanikachalam, Marimuthu Venkatesh Perumal, Natesan Srinivasan

Department of Chemistry, Annamalai University, Annamalainagar 608 002 Tamilnadu, India

ARTICLE INFO

Article history:
Received 9 May 2011
Received in revised form 29 July 2011
Accepted 10 August 2011

Keywords:
Nuclear magnetic resonance
Ab initio calculations
Photoluminescence spectroscopy
Electrical properties

ABSTRACT

Azo linked dye derivatives were synthesized and characterized by NMR, mass and elemental analysis. An excited state intramolecular proton transfer (ESIPT) in hydroxy Schiff base has been analyzed, and found that two distinct ground state isomers of I and II are responsible for the observed dual emission. DFT calculation on energy, dipole moment, charge distribution of the rotamers in the ground and excited states support the ESIPT process. PES calculation indicates that the energy barrier for the interconversion of two rotamers is too high in the excited state than the ground state. By varying the addition of base concentration to hydroxy Schiff base, two isobestic points were found which confirm the equilibrium among the *trans* enol form, anion and the *cis* enol form. Fluorescence quenching with metal ions reveal that hydroxy Schiff base can be used as a new fluorescence sensor to detect the Cu^{2+} ion.

1. Introduction

Azo compounds are versatile molecules and have received much attention in research in the view of both fundamental and applications [1,2]. Schiff base ligands are capable of forming stable complexes with metal ions and show excellent catalytic activity [3–5]. Atomic emission or mass spectroscopy (ICP-AES, ICP-MS) has been widely used for the detection of heavy metals even at very low concentrations. But these methods are relatively expensive, therefore a series of fluorescence sensors have been developed [6–10] and development of new fluorescent agents containing chelating groups can help to detect heavy metals more efficiently.

Copper exists in human body, plants and animals in trace amounts; however, high amount can cause serious health problems such as nausea, vomiting and diarrhea as well as damage to liver and kidneys [11]. Therefore, in the view of the biological and environmental importance, considerable attention has been focused on detection of Cu(II) ion [12,13] by quenching of fluorescence intensity of the employed sensing material [14–17].

Metal chelates play an essential role in living organism and a large number of metal proteins and other metal complexes of biological importance have been studied [18,19]. Because of the importance of azo-containing Schiff base compounds and in continuance of our previous studies [20], herein we report a series of azo-linked Schiff bases (**1**–**4**) and their structures were confirmed by elemental, mass, IR and NMR analysis. Photophysical studies of Schiff bases (**1**–**4**) were discussed in detail and the hydroxy Schiff base was developed as a Cu^{+2} selective fluorescence sensor. DFT calculations were carried out by using Gaussian-03 program [21,22] to supplement the experimental results.

2. Experimental

2.1. Materials and methods

Aniline (Sigma–Aldrich Ltd.), Furan-2-carboxaldehyde, Thiophene-2-carboxaldehyde, pyridine-2-carboxaldehyde, 3-hydroxypyridin-2-carboxaldehyde (S.D. fine.) and all other reagents used without further purification.

2.2. Optical measurements and computational details

NMR spectra were recorded on a Bruker 400 MHz instrument. The ultraviolet–visible (UV–vis) spectra were measured on UV–Vis spectrophotometer (Perkin Elmer, Lambda 35) and corrected for background due to solvent absorption. Photoluminescence (PL) spectra were recorded on a (Perkin Elmer LS55) fluorescence spectrometer. MS spectra were recorded on a Varian Saturn 2200 GCMS spectrometer. Quantum mechanical calculations were used to carry out the optimized geometry, NLO, HOMO–LUMO, MEP and TD-DFT with Guassian-03 program using the Becke3-Lee-Yang-Parr (B3LYP) functional supplemented with the standard 6-31G(d,p) basis set [21,22].

* Corresponding author. Tel.: +91 9443940735.
E-mail address: jtchalam2005@yahoo.co.in (J. Jayabharathi).

1386-1425/$ – see front matter © 2011 Elsevier B.V. All rights reserved.
doi:10.1016/j.saa.2011.08.017

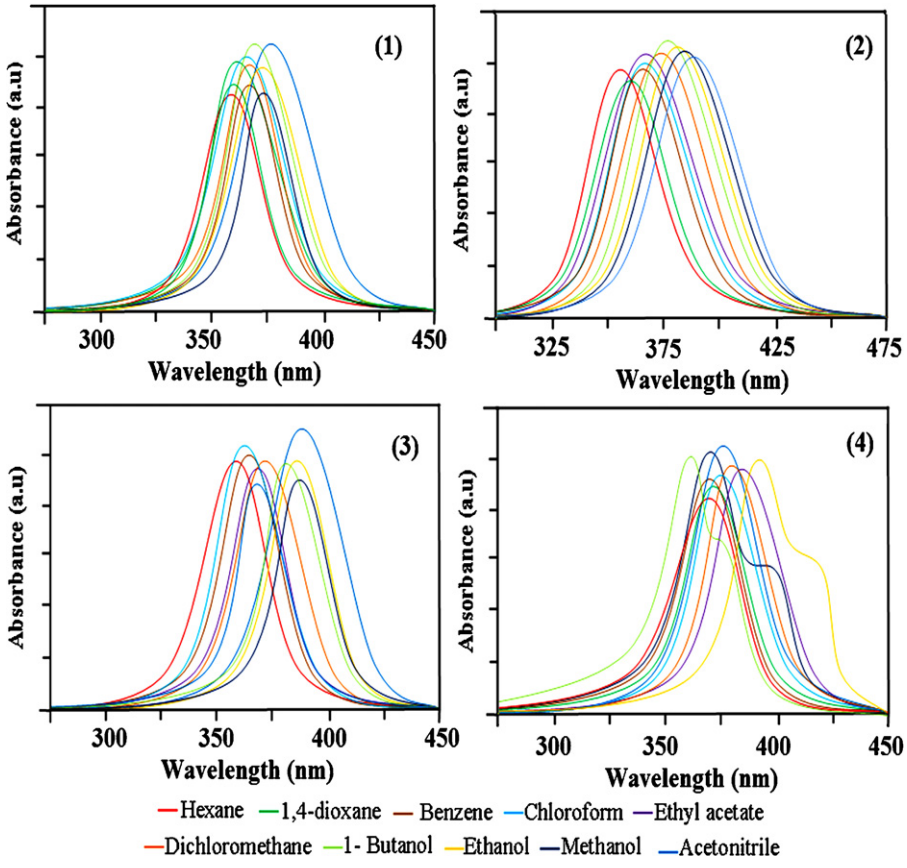

Fig. 1. Absorption spectra of Schiff bases **1**–**4**.

2.3. General procedure for the synthesis of Schiff bases

The Schiff bases (**1**–**4**) were synthesized according to the procedure reported in the literature [20]. A solution of *p*-aminoazobenzene (1 mmol) and the corresponding heterocyclic aldehydes (1.5 mmol) in 20 ml absolute ethanol were refluxed for 2 h. The resulting precipitate was filtered off and purified by column chromatography.

2.3.1. (0E,4E)-4-(2-phenyldiazenyl)-N-(2-thiophenylidene) benzenamine (*1*)

Yield: 78%, m.p: 142 °C. Anal. calcd. for $C_{17}H_{13}N_3S$: C, 70.08; H, 4.50; N, 14.42. Found: C, 69.76; H, 4.17; N, 13.75. MS: *m*/*z* 291.00, calcd. 291.08. ^{1}H NMR: 8.66 (s, 1H), 8.01 (d, 2H), 7.96 (d, 2H), 7.86 (m, 1H), 7.49–7.59 (m, 2H), 7.43 (t, 1H), 7.38 (t, 1H), 7.29 (s, 1H), 7.19 (t, 1H), 6.77 (d, 1H). ^{13}C NMR: 153.61, 153.00, 150.79, 149.58, 145.60, 142.66, 132.87, 130.85, 129.81, 129.11, 129.06, 129.01, 128.98, 125.13, 124.10, 122.81, 122.36, 121.77, 114.64.

2.3.2. (0E,4E)-4-(2-phenyldiazenyl)-N-(2-furfurylidene)benzenamine (*2*)

Yield: 78%, m.p: 137 °C. Anal. calcd. for $C_{17}H_{13}N_3O$: C, 74.17; H, 4.76; N, 15.26. Found: C, 73.46; H, 4.43; N, 14.86. MS: *m*/*z* 274.00, calcd. 275.11. ^{1}H NMR: 8.44 (s, 1H), 8.10 (s, 1H), 7.84–7.97 (m, 5H), 7.53–7.45 (m, 4H), 7.29 (s, 1H), 6.77 (d, 1H). ^{13}C NMR: 152.76, 129.34, 129.08, 128.97, 125.12, 124.78, 124.75, 124.03, 123.90, 123.79, 122.99, 117.01, 116.96, 116.56, 114.63.

2.3.3. (0E,4E)-4-(2-phenyldiazenyl)-N-(2-pyridylidene)benzenamine (*3*)

Yield: 87%, m.p: 116 °C. Anal. calcd. for $C_{18}H_{14}N_4$: C, 76.17; H, 5.43; N, 13.32. Found: C, 75.50; H, 4.93; N, 19.57. MS: *m*/*z* 285.00, calcd. 286.12. ^{1}H NMR: 8.77 (bd, 1H), 8.69 (s, 1H), 8.04 (m, 1H), 7.41–7.45 (m, 3H), 7.49–7.52 (m, 2H), 7.53–7.57 (m, 2H), 7.84–7.88 (m, 3H), 7.96 (m, 1H). ^{13}C NMR: 161.41, 154.35, 153.31, 153.00, 152.75, 149.59, 145.59, 137.07, 136.76, 130.96, 129.86, 129.80, 129.11.

2.3.4. (0E,4E)-4-(2-phenyldiazenyl)-N-(o-hydroxypyridylidene) benzenamine (*4*)

Yield: 83%, m.p: 123 °C. Anal. calcd. for $C_{18}H_{14}N_4O$: C, 70.35; H, 4.67; N, 18.53. Found: C, 70.15; H, 4.23; N, 17.98. MS: *m*/*z* 301.00, calcd. 302.12. ^{1}H NMR: 8.51 (s, 1H), 8.01 (s, 1H), 7.45–7.93 (m, 5H), 7.45–7.53 (m, 4H), 7.39 (s, 1H), 6.97 (d, 1H), 4.91 (s, 1H). ^{13}C NMR: 155.67, 152.32, 151.75, 140.12, 139.47, 131.32, 129.46, 127.53, 124.11, 122.79.

3. Results and discussion

3.1. Photophysical characterization of (*1*–*4*)

The UV–vis spectra of the Schiff bases (**1**–**4**) were recorded in protic and aprotic solvents in the region 200–500 nm, the band appeared around 380.0 nm in dioxane is due to π–π* transition (Fig. 1). Since in aminobenzene dyes, n–π* and π–π* transitions are in close proximity, the low intensity n–π* transition is completely overlaid by the intensive π–π* transition [23,24]. The absorption spectra largely depend on the solvent polarity and red shift was observed in hydroxyl solvents. Larger red shift in the absorption

Table 1
Photoluminescence spectral data of various solvents and solid emission spectra of picrate derivatives **1**–**4**.

Solvent	Absorption[a] (λ, nm)				Emission[b] (λ, nm)				Stokes shift (cm^{-1})			
	1	**2**	**3**	**4**	**1**	**2**	**3**	**4**	**1**	**2**	**3**	**4**
n-Hexane	362	357	360	371	402	407	419	413	2749	3441	3911	2741
1,4-Dioxane	368	365	368	372	415	417	423	413	3078	3416	3533	2669
Benzene	364	360	365	371	412	414	421	423, 480	3201	3623	3644	3314
Chloroform	369	368	367	375	423	426	428	414	3460	3700	3883	2512
Ethyl acetate	370	369	371	385	427	429	430	427	3608	3790	3698	2555
Dichloromethane	372	374	373	376	428	434	432	418	3517	3696	3662	2672
Butanol	370	377	378	361, 401	427	435	434	441	3608	3537	3414	2262
Ethanol	374	381	383	392, 420	428	437	436	440	3373	3363	3174	1082
Methanol	375	383	384	370, 400	432	436	437	439	3519	3174	3158	2221
Acetonitrile	379	387	388	375.6	434	438	440	424	3344	3009	3046	3039

[a] UV–Vis absorption measured in solution concentration = 1×10^{-5} M.
[b] Photoluminescence measured in solution concentration = 1×10^{-4} M.

band (Table 1) may be due to the stabilizing interaction between the hydroxyl group of the alcohol and the hetero atoms (N, S, O) of the Schiff bases.

The absorption spectra for the yellowish colour solution of hydroxy Schiff base (**4**) in neutral ethanol show band at 392 nm along with a shoulder at 420 nm. Addition of different concentrations of NaOH [0–0.017 M] to the ethanol solutions of **4** resulted in a single band at 400 nm at the expense of both 392 and 420 nm bands with two isobestic points around 360 and 410 nm. In hexane, the absorption spectrum of **4** shows a single band at 371 nm. Therefore, the absorption band at 392 nm can be safely assigned to the intramolecularly hydrogen bonded enol form, 400 nm is assigned to the anion and 420 nm is due to the *cis* enol form of **4**, respectively, and the isobestic points confirm the equilibrium among the *trans* enol form, anion and the *cis* enol form (Fig. 2).

All Schiff bases (**1**–**4**) fluoresce strongly at room temperature (Table 1), the emission spectrum (Fig. 3) for the yellowish colour solution of **4** in neutral ethanol shows a band at 445 nm. The emission is switched 'On' with decreasing pH, because at low pH the hydroxyl oxygen is protonated, its oxidation potential raised which switches fluorescence 'On' and at high pH, the intensity of fluorescence emission is low, i.e., switched 'Off' due to anion formation which quenches fluorescence.

The solid state UV–vis spectra of Schiff bases **1**–**4** exhibit absorbance (λ_{max}) at 544, 550, 568 and 560. The optical band gap value of Schiff bases **1**–**4** are found to be 2.27, 2.25, 2.18 and 2.21 eV, respectively, and these are smaller than the previously reported Schiff base [25]. The smaller band gap indicates easy electronic transitions from bulk to vacuum energy level of the compounds and these compounds have high electrical conductivity as well as fluorescence property. The higher Stokes's shift value (Table 1) supplies very low background signals and resultantly allows the usage of the material in construction of a fluorescence sensor [26]. As seen in Table 1 in comparison with the other solvents, benzene solution of **4** has larger Stokes shift value than other solvents, indicates that the usage of **4** as an ion selective sensor in benzene solution.

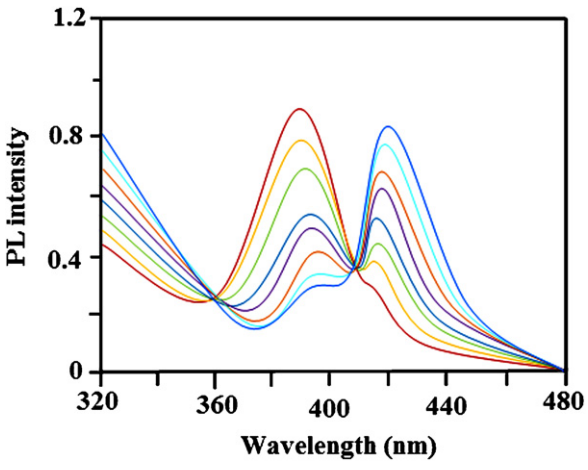

Fig. 2. Absorption spectrum of Schiff base (**4**) in ethanol in the presence of sodium hydroxide ([NaOH] = 0–0.017 M).

The changes in the fluorescence properties of **4** caused by different metal ions such as Co^{2+}, Hg^{2+}, Ni^{2+} and Cu^{2+} were measured in ethanol. The fluorescence of **4** quenched markedly with the gradual addition of Cu^{2+} but the fluorescence properties of **4** were influenced by other metal ions (Fig. 4a). The fluorescence intensity of **4** was linearly reduced with increase in concentration of Cu^{2+} (Fig. 4b). According to these spectra when the Cu^{2+} concentrations are 5×10^{-3} and 5×10^{-5} mol/L the relative intensity changes ($I_0 - I/I_0$) are 0.88 and 0.30, respectively (Fig. 5). The quenching in fluorescence intensity of Schiff base by the addition of Cu^{2+} cation indicates the complexation of Schiff base with Cu^{2+}, the Schiff base has bidentate sites and forming the expected Cu^{2+} complex (Fig. S1) [25,27]. The possible reason for the fluorescence quenching is the formation of a ground state non-fluorescent complex and the enhancement of spin–orbit coupling [28] for **4**–Cu^{2+} is presumed resulting in the fluorescence quenching and the observed linear regression equation is, $(I_0 - I/I_0) = -0.163 - 0.196 \log[Cu^{2+}]$ where, I_0 is the emission intensity of Cu^{2+} free Schiff base, I is the fluorescence intensity of the Schiff base (**4**) in the presence of metal ion Cu^{2+}, $[Cu^{2+}]$ is the concentration of metal ion and the correlation co-efficient is 0.992. According to the obtained results, Schiff base (**4**) can be used as a new fluorescence sensor to detect the quantity of Cu^{2+} ion in any sample solution depending on the relative intensity change.

3.2. Excited state intramolecular proton transfer (ESIPT) process PES studies

Hydroxy Schiff base (**4**) exists as intramolecular hydrogen bonded isomers namely *trans* enol I and *cis* enol II in aprotic solvents (Fig. S2(a)). Excitation of the *trans* enol isomer I should lead to the formation of the keto-isomer III due to ESIPT (Fig. S2(b)). But, we found out that the fluorescence spectrum in dioxane contains two emission bands at shorter wavelength (423 nm) are assigned to isomer I and the small shoulder peak at higher wavelength 480 nm reveals that only the isomer II of **4**. However in alcoholic solvent, a short wavelength emission band appears which may be due to the presence of intermolecular hydrogen bonding with solvent molecule leading to the stabilization of solvated isomer IV in which ESIPT is impossible [29].

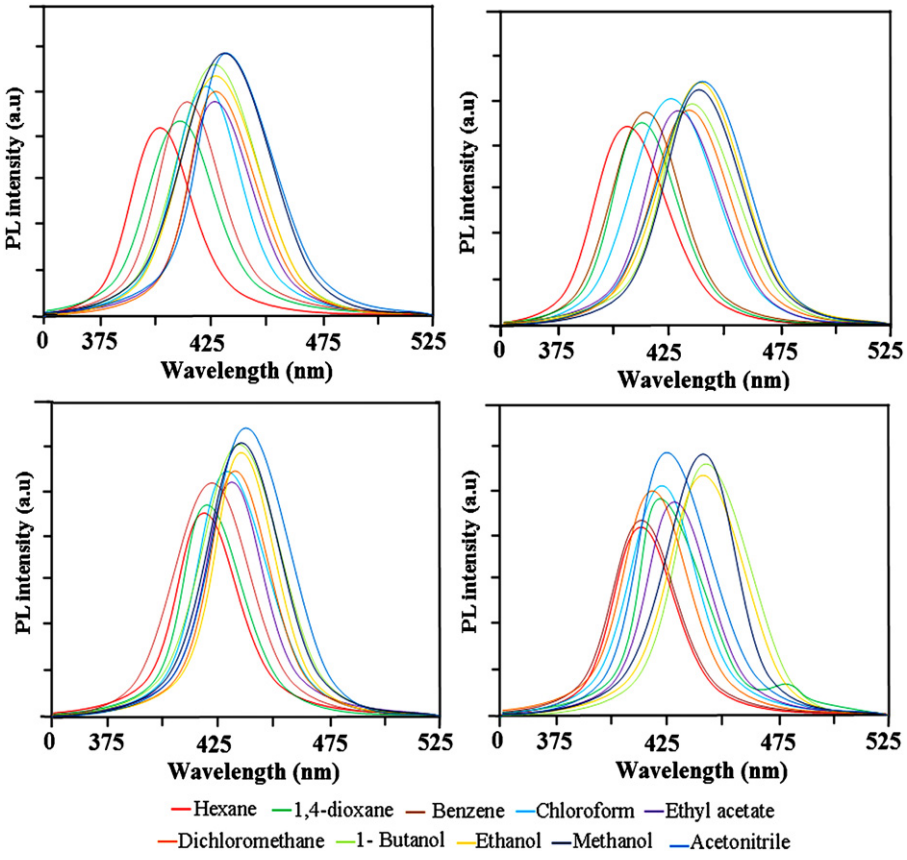

Fig. 3. Emission spectra of Schiff bases **1**–**4**.

Table 2
Relative energies[a] (kcal/mol), electron density and dipole moments (*D*) in the ground and excited state for rotamers I, II and III of Schiff base (**4**).

Compound	Rotamers	Electron density		Ground state		Excited state	
		N(24)	O(36)	μ (*D*)	*E* (kcal/mol)	*E* (kcal/mol)	μ (*D*)
	I	−0.462 (−0.523)[b]	−0.531 (−0.501)[b]	4.16	1.10 (0.00)	108.00 (91.26)	9.02
4	II	–	–	3.30	2.21 (0.82)	112.28 (100.57)	8.26
	III	0.431	−0.592	5.80	16.23 (8.60)	96.08 (350.82)	5.92

[a] Relative energies are calculated with respect to the ground state minimum energy form in ethanol. Values in the parenthesis are recorded in ethanol.
[b] Excited state isomer I.

DFT calculation was carried out for better understanding the ESIPT mechanism. The keto and enol isomers in the ground and the excited states (Table 2) reveal that excitation of *trans* enol isomer (**I**) leads to an increase in the electron density at N(24) atom and decrease at O(36) atom resulting in ESIPT and formation of the excited keto isomer in excited state which emits luminescence and returns to the ground state keto form and is characterized by a large positive charge at the N(24) atom and negative charge at the O(36)

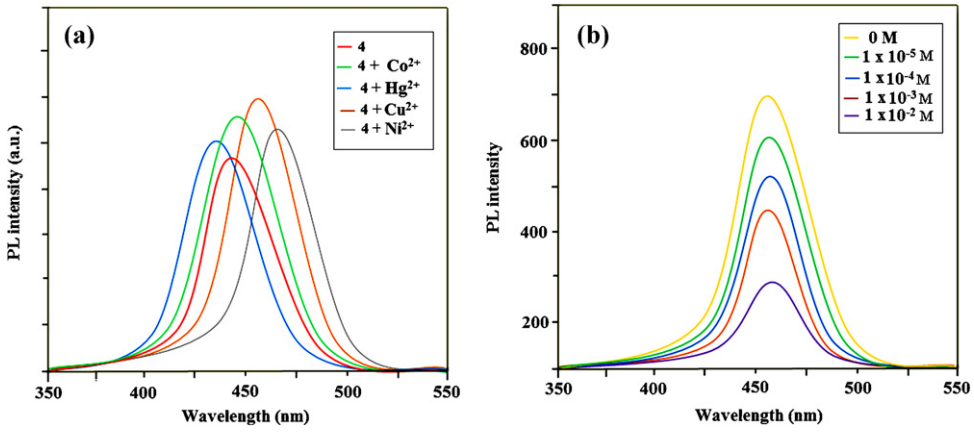

Fig. 4. (a) Fluorescence spectra of Schiff base (**4**) in the presence of various metal ions. (b) Fluorescence chemosensors blocking by metal ion binding.

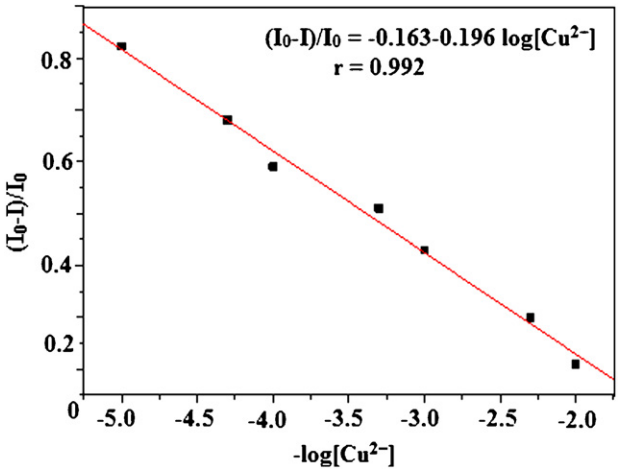

Fig. 5. Plot of normalized intensity ($I_0 - I/I_0$) against concentration for Cu^{2+} ion.

atom. As a result, a reverse process occurs in the ground state of the molecule producing an initial molecule in the enol form.

The ESIPT process was explained by large number of theoretical calculations [30–32]. The ground, excited state energies (CIS) and dipole moment of the three species I, II and III were calculated using DFT/6-31G(d,p) method. The barrier for interconversion of I and II in the ground state is 4.81 kJ/mol (Isolated molecule) and 4.64 kJ/mol (EtOH) and for the excited state 17.89 kJ/mol (Isolated molecule) and 14.92 kJ/mol (EtOH), respectively. The barriers for interconversion in the excited state are much higher than that in the ground state (Table 2).

3.3. Hyperpolarizability of Schiff bases *1*–*4* by DFT method

The HOMO–LUMO energy gap (Fig. 6) 7.61 (**1**), 7.65 (**2**), 7.70 (**3**) and 7.76 (**4**) kcal/mol was calculated by B3LYP/6-31G(d,p), which confirmed the eventual charge transfer interactions within the molecule. Table 3 implies that Schiff bases are highly polar having non-zero dipole moment and hence have well microscopic NLO behaviour [30]. To determine the transference region and hence to know the suitability of **1**–**4** for microscopic nonlinear optical applications, the UV–vis spectral studies have been taken for discussion. The increased transparency in the visible region (π–π^* transition) might enable the microscopic NLO behaviour with non-zero values [31]. The β values (Table 3) computed here might be correlated with UV–vis spectroscopic data in order to understand the molecular structure and NLO relationship in view of a future optimization of the microscopic NLO properties. The band at around 370.0 nm exhibits a solvatochromic shift, characteristic of a large dipole moment (Table 3) and frequently suggestive of a large hyperpolarizability (Table 3). These compounds show red shift in absorption with increasing solvent polarity, accompanied with the upward shifts non-zero values in the β-components have large hyperpolarizabilities and hence have rather well microscopic NLO behaviour [32].

3.4. Conformation of Schiff bases *1*–*4*

Comparison of the chemical shifts of azomethine proton in the Schiff bases **1**–**4** with that of aldehydic proton in their corresponding substituted benzaldehydes reveals that considerable shielding has been observed due to the conversion of aldehydes to Schiff bases. Generally in Schiff bases, the bulky group adopts *trans* orientation. Therefore, it is inferred that the azomethine proton is *syn* to diazenophenyl benzenamine ring in Schiff bases **1**–**4**. Therefore, the favoured conformation of the Schiff bases **1**–**4** is predicted to be the *anti* conformation, i.e., the CH=N and N=N groups are anti to each other.

Generally in the Schiff base derived from *p*-aminoazobenzene, two possible conformations (Fig. 7) with respect to the CH=N and N=N groups are shown. In the planar *anti* conformation, the CH=N bond and N=N bond are *trans* to each other whereas in the planar *syn* conformation, the CH=N bond and N=N bond

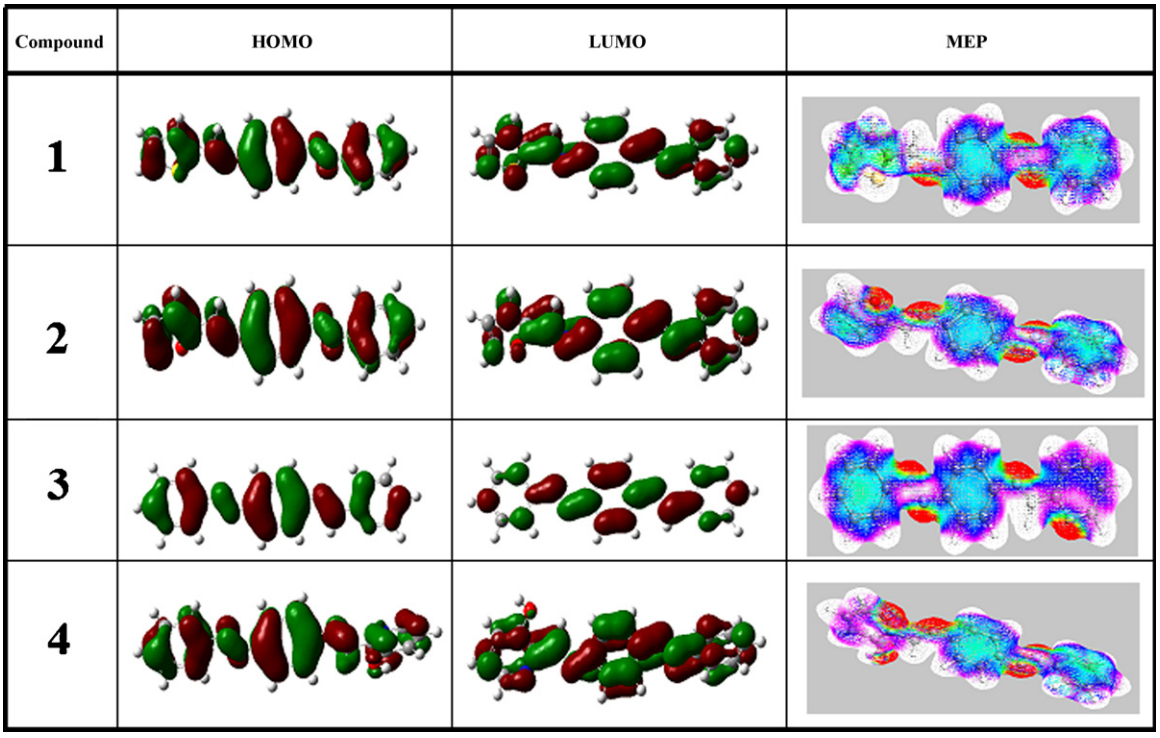

Fig. 6. HOMO–LUMO molecular orbitals and MEP surfaces of **1**–**4**.

Table 3
Electric dipole moment (D), polarizability (α) and hyperpolarisability (β_{total}) of **1–4** calculated by B3LYP/6-31G(d,p).

Parameter	1	2	3	4
Dipole moment (D)				
μ_x	−0.6457	−1.2857	0.1837	0.1812
μ_y	0.0316	−0.1463	−0.0019	−0.2680
μ_z	0.1474	−0.1487	0.2884	0.6879
μ_{tot}	−0.4667	−1.5807	0.4702	0.6011
Polarizability (α)				
α_{xx}	5.6528	4.9652	7.2654	2.2658
α_{xy}	7.2352	5.6354	9.9605	6.2568
α_{yy}	1.9651	1.9632	4.7011	2.3698
α_{xz}	−2.1235	−2.8652	−3.8453	−1.2568
α_{yz}	−3.0231	−4.1256	−6.9998	−3.2365
α_{zz}	2.9856	1.3215	5.3716	2.1258
$\alpha_{tot} \times 10^{-25}$	5.2381	4.0754	8.5650	3.3401
Hyperpolarisability (β)				
β_{xxx}	−0.1390	−0.2142	−0.0566	−0.1891
β_{xxy}	0.0666	0.0938	0.0164	−0.0818
β_{xyy}	−0.0600	−0.0768	−0.0176	−0.0706
β_{yyy}	0.0142	−0.0242	0.0043	0.0074
β_{xxz}	0.2438	−0.0102	0.2672	0.2412
β_{xyz}	−0.2210	−0.0884	−0.0924	0.2377
β_{yyz}	0.3513	0.0799	0.2269	0.3576
β_{xzz}	0.2673	−0.0203	−0.2385	0.2604
β_{yzz}	0.2948	0.0600	−0.2479	−0.3042
β_{zzz}	1.2109	0.3030	0.6093	1.2436
$\beta_{tot} \times 10^{-33}$	15.947	4.3421	10.1006	16.2522

are *cis* to each other. Therefore, these two conformations are labelled as *anti* and *syn* conformations, respectively. The favoured conformation of all the Schiff bases (**1–4**) were predicted as *anti* by DFT/B3LYP-631G(d,p) method.

The MEP map shows that oxygen and nitrogen atoms represent the most negative potential region but the nitrogen atom seems to exert comparatively small negative potential as compared to oxygen atom. The hydrogen atom attached to the six and five membered ring bear the maximum positive charge. The Mulliken charge distribution (Fig. 8) reveals that when compared to nitrogen atoms N12, N13 and N24, N24 is considered as more basic site, which also support the proton migration from hydroxy group (**4**) to N24 atom (ESIPT). The charge distribution shows that the more negative charge is concentrated on oxygen atom whereas the partial positive charge resides at hydrogens.

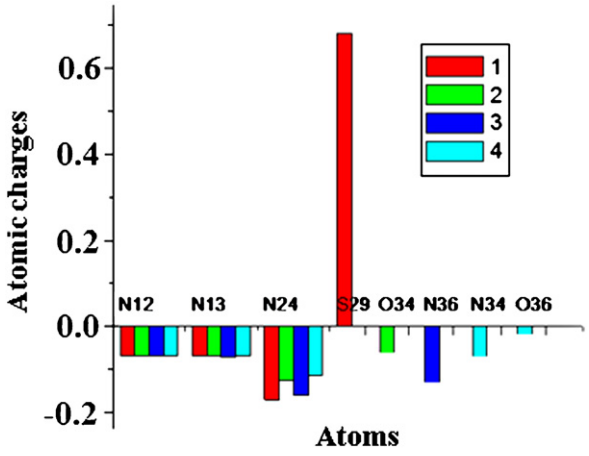

Fig. 8. Mulliken atomic charges for Schiff bases **1–4**.

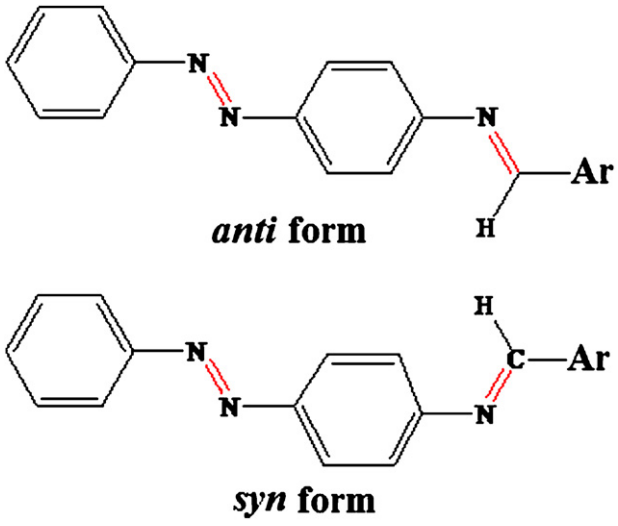

Fig. 7. *Syn* and *anti* conformers of Schiff base (**4**).

4. Conclusion

Photophysical aspects of Schiff bases derived from heterocyclic aldehydes and ESIPT process in hydroxy Schiff base have been studied in detail. The fluorescence quenching studies of hydroxy Schiff base implies that it can be used as a new fluorescence sensor to detect the Cu^{2+} ion. PES calculation reveals the barrier for interconversion in the excited state is much higher than that in the ground state. The non-zero dipole moment values show that these compounds are highly polar molecules and have microscopic NLO behaviour. Its electric dipole moments, polarizability, hyperpolarisability, HOMO–LUMO energies and MEP studies were determined by DFT calculation.

Acknowledgments

One of the author Dr. J. Jayabharathi, Associate Professor in Chemistry, Annamalai University is thankful to Department of Science and Technology [No. SR/S1/IC-73/2010] and University Grants commission (F. No. 36-21/2008 (SR)) for providing funding to this research work.

Appendix A. Supplementary data

Supplementary data associated with this article can be found, in the online version, at doi:10.1016/j.saa.2011.08.017.

References

[1] K. Nejati, Z. Rezvani, B. Massoumi, Dyes Pigments 75 (2007) 653–657.
[2] E. Peker, S. Serin, Synth. React. Inorg. Met.-Org. Chem. 34 (2004) 859–864.
[3] P. Souza, J.A. Garcia-Vazquez, J.R. Masaguer, Transit. Met. Chem. 10 (1985) 410–412.
[4] H. Naeimi, J. Safari, A. Heidarnezhad, Dyes Pigments 73 (2007) 251–257.
[5] S.J. Lippard, J.M. Berg, Principles of Bioinorganic Chemistry, University Science Books, California, 1994.
[6] Y.W. Wang, Y.T. Shi, Y. Peng, A.J. Zhang, T.H. Ma, W. Dou, J.R. Zheng, Spectrochim. Acta A 72 (2009) 322–326.
[7] N. Shing, N. Kaur, J. Dunn, M. MacKay, J.F. Callan, Tetrahedron Lett. 50 (2009) 953–956.
[8] O. Oter, K. Ertekin, R. Kilincarslan, M. Ulusoy, B. Cetinkaya, Dyes Pigments 74 (2007) 730–735.
[9] L. Guo, S. Hong, X. Lin, Z. Xie, G. Chen, Sens. Actuators B 130 (2008) 5010–5011.
[10] G. Farrugia, S. Lotti, L. Prodi, N. Zaccheroni, M. Montalti, P.B. Savage, G. Andreani, V. Trapani, F.I. Wolf, J. Fluoresc. 19 (2009) 11–19.
[11] N. Aksuner, E. Henden, I. Yilmaz, A. Cukurovali, Sens. Actuators B 134 (2008) 510–515.
[12] G.K. Li, Z.X. Xu, C.F. Chen, Z.T. Huang, Chem. Commun. 15 (2008) 1774–1776.
[13] V. Dujols, F. Ford, A.W. Czarnik, J. Am. Chem. Soc. 119 (1997) 7386–7387.
[14] H.J. Kim, S.Y. Park, S. Yoon, J.S. Kim, Tetrahedron 64 (2008) 1224–1230.
[15] H.L. Mu, R. Gong, Q. Ma, Y.M. Sun, E.Q. Fu, Tetrahedron Lett. 48 (2007) 5525–5529.
[16] J. Xie, M. Menand, S. Maisonneuve, R. Metivier, J. Org. Chem. 72 (2007) 5980–5985.
[17] Y.J. Mei, P.A. Bentley, W. Wang, Tetrahedron Lett. 47 (2006) 2447–2449.
[18] M. Kurtog'lu, E. Ispir, S. Serin, Dyes Pigments 77 (2008) 75–81.
[19] E. Ispir, Dyes Pigments 82 (2009) 13–19.
[20] J. Jayabharathi, V. Thanikachalam, K. Jayamoorthy, M. Venkatesh Perumal, Spectrochim. Acta A 79 (2011) 6–16.
[21] Guassian 03 Program, Gaussian Inc., Wallingford, CT, 2004.
[22] H.B. Schlegel, J. Comput. Chem. 3 (1982) 214–218.
[23] J. Jayabharathi, V. Thanikachalam, N. Srinivasan, M. Venkatesh Perumal, K. Jayamoorthy, Spectrochim. Acta A 79 (2011) 137–147.
[24] G. Gabor, Y.F. Frei, E. Fischer, J. Phys. Chem. 72 (1968) 3266–3272.
[25] K. Das, N. Sarkar, A.K. Ghosh, D. Majumdar, D.N. Nath, K. Bhattacharyya, J. Phys. Chem. 98 (1994) 9126–9132.
[26] P.F. Barbara, P.K. Walsh, L.E. Brus, J. Phys. Chem. 93 (1989) 29–34.
[27] G.J. Woolfe, M. Melzig, S. Schneider, F. Dorr, Chem. Phys. 77 (1983) 213–221.
[28] A.L. Sobolewski, Chem. Phys. Lett. 211 (1993) 293–301.
[29] H. Unver, A. Karakas, A. Elmali, J. Mol. Struct. 702 (2004) 49–54.
[30] I.S. Lee, D.M. Shin, Y. Yoon, S.M. Shin, Y.K. Chung, Inorg. Chim. Acta 343 (2003) 41–50.
[31] S.G. Prabhu, P.M. Rao, S.I. Bhat, V. Upadyaya, S.R. Inamdar, J. Cryst. Growth 233 (2001) 375–379.
[32] F. Volmer, W. Rettig, J. Photochem. Photobiol. A: Chem. 95 (1996) 143–155.